Electron drift velocity in lattice-matched AlInN/AlN/GaN channel at high electric fields
— **Source link** ⧉

L. Ardaravičius, M. Ramonas, J. Liberis, O. Kiprijanovic ...+5 more authors

Institutions: Virginia Commonwealth University

Related papers:

- Hot phonons in GaN channels for HEMTs

- Power electronics on InAlN/(In)GaN: Prospect for a record performance

- Subpicosecond time-resolved Raman studies of LO phonons in GaN: Dependence on photoexcited carrier density

- High electron mobility in nearly lattice-matched AlInN∕AlN∕GaN heterostructure field effect transistors

- Handbook of Nitride Semiconductors and Devices

2009

Electron drift velocity in lattice-matched AlInN/ AlN/GaN channel at high electric fields

L. Ardaravičius
Semiconductor Physics Institute

M. Ramonas
Semiconductor Physics Institute

J. Liberis
Semiconductor Physics Institute

See next page for additional authors

Authors

L. Ardaravičius, M. Ramonas, J. Liberis, O. Kiprijanovič, A. Matulionis, J. Xie, M. Wu, J. H. Leach, and H. Morkoç

Electron drift velocity in lattice-matched AlInN/AlN/GaN channel at high electric fields

L. Ardaravičius,[1,a)] M. Ramonas,[1] J. Liberis,[1] O. Kiprijanovič,[1] A. Matulionis,[1] J. Xie,[2] M. Wu,[2] J. H. Leach,[2] and H. Morkoç[2]

[1]*Fluctuation Research Laboratory, Semiconductor Physics Institute, A. Goštauto 11, Vilnius 01108, Lithuania*

[2]*Department of Electrical and Computer Engineering, Virginia Commonwealth University, Richmond, Virginia 23284, USA*

Hot-electron transport was probed by nanosecond-pulsed measurements for a nominally undoped two-dimensional channel confined in a nearly lattice-matched $Al_{0.82}In_{0.18}N/AlN/GaN$ structure at room temperature. The electric field was applied parallel to the interface, the pulsed technique enabled minimization of Joule heating. No current saturation was reached at fields up to 180 kV/cm. The effect of the channel length on the current is considered. The electron drift velocity is deduced under the assumption of uniform electric field and field-independent electron density. The highest estimated drift velocity reaches $\sim 3.2 \times 10^7$ cm/s when the AlN spacer thickness is 1 nm. At high fields, a weak (if any) dependence of the drift velocity on the spacer thickness is found in the range from 1 to 2 nm. The measured drift velocity is low for heterostructures with thinner spacers (0.3 nm). © *2009 American Institute of Physics*. [doi:10.1063/1.3236569]

I. INTRODUCTION

Nitride heterostructures have attracted much attention because of their potential use in high-power and high-frequency electronic devices.[1] In the absence of intentional doping, a two-dimensional electron gas (2DEG) (with a typical density in excess of 10^{13} cm^{-2}) forms at the heterointerface due to spontaneous and piezoelectric polarization.[2] The $Al_{1-x}In_xN$ alloy can be grown lattice matched (LM) to GaN for an indium content close to 17%–18%.[3] Thus, the material issues due to strain and its relaxation can be avoided in the LM AlInN/GaN heterojunctions, and a high 2DEG density is reached solely due to the spontaneous polarization.[4] These properties, together with high mobility and low sheet resistance, make the LM structures ideal for the realization of a heterostructure field effect transistor (HFET).[4–9]

Insertion of a thin AlN spacer between the AlInN and GaN layers helps to reduce remote alloy scattering and achieve high electron mobility.[10,11] The optimum spacer thickness is around 1 nm.[10,12,13] A thicker AlN spacer may cause mobility degradation when surface roughness increases during the growth.[11] It seems that the quality of the AlInN layer degrades if specific structural defects are created at the AlN/AlInN interface when the spacer is too thick, probably due to plastic relaxation.[14] An onset of mobility degradation due to the increased surface roughness was obtained for AlN thicknesses larger than 5 nm in pure ultrathin AlN/GaN structures.[15]

Hot-electron transport at high electric fields was investigated experimentally and/or theoretically in bulk GaN[16–28] and different nitride heterostructures: AlGaN/GaN,[23,29,30] AlGaN/AlN/GaN,[31] AlGaN/GaN/AlN/GaN,[32] and LM AlInN/AlN/GaN.[33] In the AlInN/AlN/GaN structure, the

electron drift velocity is measured for 100 ns voltage pulses at fields up to 70 kV/cm. The electric field range can be extended if pulses from one to a few nanoseconds are employed.[25,31]

The main aim of this paper is to report on high-field electron transport experiments for the LM $Al_{0.82}In_{0.18}N/AlN/GaN$ under conditions of minimized Joule effect in order to analyze the effect of the AlN spacer thickness on the electron drift velocity.

II. SAMPLES

The LM $Al_{0.82}In_{0.18}N/AlN/GaN$ structures were grown in a vertical low-pressure metal-organic chemical vapor deposition system.[10] The heterostructures consisted of a 4 μm thick GaN buffer layer on a 2 in. (0001) sapphire substrate, an undoped pseudomorphic 0.3–2 nm AlN spacer, and a 17–20 nm thick undoped $Al_{0.82}In_{0.18}N$ layer covered with a 1–2 nm GaN cap layer. The 2DEG channel was located in the GaN layer close to the AlN spacer. A degenerate 2DEG, $n_{2D} = (1.2-1.5) \times 10^{13}$ cm^{-2}, was induced by spontaneous polarization (see Table I). The low-field mobility was

TABLE I. Measured low-field mobility and sheet carrier density for $Al_{0.82}In_{0.18}N/AlN/GaN$ structures at room temperature.

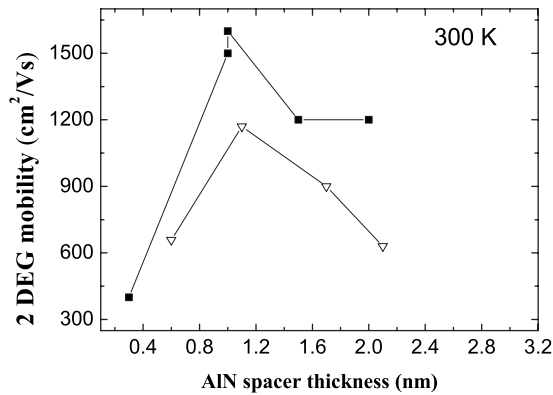| Structure (nm)	Cap layer (nm)	AlN spacer (nm)	μ_0 (cm^2/V s)	n_{2D} ($\times 10^{13}$ cm^{-2})
1656	2	1	1500	1.2
2061	1	1.5	1200	1.5
2073	1	1	1600	1.2
2081	1	0.3	400	1.4
2083	1	2	1200	1.4

a)Electronic mail: linas@pfi.lt.

FIG. 1. Room temperature mobility vs the AlN spacer thickness for LM AlInN/AlN/GaN: present work (squares), Ref. 11 (inverted triangles).

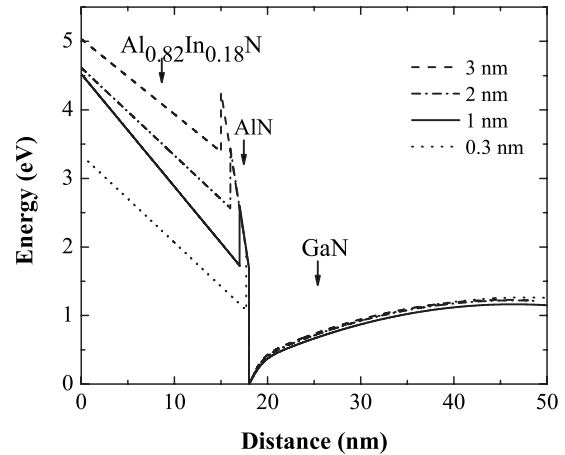FIG. 2. Potential profile for the $Al_{0.82}In_{0.18}N/AlN/GaN$ channel at room temperature. The dashed, dash-dotted, solid, and dotted lines indicate the spacer thickness of 3, 2, 1, and 0.3 nm, respectively.

$\mu_0 = 400 - 1600$ cm^{-2}/V s at room temperature; its dependence on the AlN spacer thickness is illustrated in Fig. 1 (squares).

The free-electron density profile in a 2DEG channel can be obtained from the solution of coupled Schrödinger and Poisson equations.[34] For a LM AlInN/AlN/GaN structure, the calculated polarization-induced charge density σ/e (σ is the polarization-induced charge, and e is the electron charge) is negative at the AlInN/AlN interface (-4.3×10^{13} cm^{-2}), and the charge density is positive between AlN and GaN layers (6.8×10^{13} cm^{-2}). The resultant fixed polarization-induced charge is positive, and free electrons tend to compensate it. This causes the formation of 2DEG in the GaN layer near the interface. Thus, the spontaneous polarization alone induces the 2DEG of $\sim 2.5 \times 10^{13}$ cm^{-2} in the LM $Al_{1-x}In_xN/AlN/GaN$.[4,11–13,35–37]

Our calculations assume additional negative charge accumulated on the AlGaN surface to account for the surface states occupied by electrons. The negative residual acceptor charge is also introduced in the GaN buffer for a better 2DEG confinement. These calculations lead to the resultant 2DEG density close to the values given in Table I.

At a low density of electrons, the charge of free electrons can be ignored and the confining potential can be approximated by a simple triangular function. However, for a high-density 2DEG, this approximation is rather poor, and the Schrödinger equation should be solved self-consistently together with the Poisson equation.[38,39]

The conduction band potential profile for different AlN spacer thicknesses (0.3, 1 2, and 3 nm) at zero electric field and 300 K temperature is shown in Fig. 2. The highest energy barrier belongs to the 3 nm thick spacer layer.

It follows from the low-field mobility results (Table I and Fig. 1) and the calculations of the 2DEG density and of the potential profile (Fig. 2) that a 0.3 nm spacer is too thin for the 2DEG confinement and good transport performance at low electric fields. On the other hand, a 1 nm spacer seems to be of the optimal thickness: remote alloy scattering is reduced and the electrons are kept confined at the AlN/GaN interface.

Two-electrode samples for hot-electron transport measurements had an electrode width $w = 275$ μm and channel lengths: $L = 5, 7, 9.1, 13.2,$ and 15.2 μm. Coplanar Ohmic Ti/Al/Ni/Au electrodes were annealed at 1120 K. The contact resistance R_c was estimated from the dependence of the sample resistance on the channel length measured at low electric fields: R_c varied from 3.6 to 16.3 Ω. No asymmetry of the current was observed in the investigated range of applied voltages (the asymmetry often results from the voltage-dependent contact resistances).

III. EXPERIMENT

Hot-electron experiments were carried out for LM $Al_{0.82}In_{0.18}N/AlN/GaN$ channels using a nanosecond-pulsed technique.[40] Electric field E was applied in the interface plane [here $E = (U - IR_c)/L$, where U is the applied voltage and I is the current flowing through the sample]. The effect of the channel Joule heating on the current has been minimized.[29]

The high voltage pulses were formed in an electrical circuit that consisted of a dc voltage source, a mercury-wetted relay, and a charged coaxial line. The high voltage pulse amplitude was determined by the dc source and adjusted by power attenuators. When the coaxial line was discharged through the relay, the electric pulse reached the sample through the delay line, and the transmitted signal was fed into a 0–5 GHz bandwidth storage sampling oscilloscope through a wide band switch, a tee, and fixed thin film attenuators. A high-frequency gauge resistor is used for calibration.

The electrical circuit can be described by a simple equivalent circuit of three resistors connected in series: the internal resistance of the generator (50 Ω), the sample resistance, and the oscilloscope input resistance (50 Ω). Therefore, the current through the sample, I, is equal to $U_{osc}/(50 \ \Omega)$, where U_{osc} is the registered voltage of the transmitted pulse amplitude. The voltage drop U through the sample is equal to $U_{dc} - 2U_{osc}$, where U_{dc} is the dc source voltage. The value of U_{dc} is calculated from the signal transmitted through the ideal (gauge) resistor of known resistance R_G: $U_{dc} = 2U_{Gosc}(R_G/100 + 1)$, where U_{Gosc} is the registered voltage of the signal transmitted through the gauge resistor. Figure 3 shows snapshots of the signals on the oscilloscope screen for the sample and the gauge resistor. The pulse rise
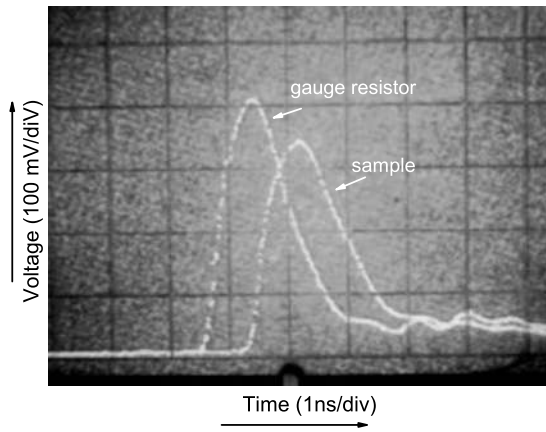
FIG. 3. Snapshots of the signal for structure 1656 and the ideal (gauge) resistor. The electric field strength is 66 kV/cm, the deflection factor is 0.1 V/div, and the sweep range is 1 ns/div.

times for the both devices are of the order of ~0.5 ns. Consequently, the sample RC makes a negligible influence on the signal shape.

At high fields, samples suffered soft damage from time to time. The damage was estimated according to the change in the zero-field resistance measured before and after the high-field experiments. This paper presents the results for the samples when the damage is less than 5%.

IV. EXPERIMENTAL RESULTS

Our task is to measure the dependence of current on the applied electric field in the $Al_{0.82}In_{0.18}N/AlN/GaN$ channel at room temperature for structures with the different spacer thicknesses.

First, to determine whether the investigated structures are homogeneous, the dependence of current on the average electric field is illustrated for sample A (Fig. 4, bullets) and sample B (open circles) cut from different places of the same wafer (2073). The current values differ by 10% at fields near 20 kV/cm and 25% at 170 kV/cm. Second, the optimum channel length is considered. Figure 5 shows the current as a function of electric field for the channels of different lengths. Samples with a channel length greater than 9 μm survived 1 ns pulses of the electric field $E<100$ kV/cm. The dependence on the channel length is weak if any: the values of

FIG. 5. Dependence of current on the electric field for structure 1656 at room temperature. The channel lengths are $L=7$ μm (bullets), 9.1 μm (open squares), 13.2 μm (open triangles), and 15.2 μm (closed triangles). The voltage pulse duration is 3 ns.

current and voltage are scattered within $\pm10\%$ range. From this we conclude that the nonuniformity of the electric field is not essential.

No tendency for the current to saturate is observed at $E<150$ kV/cm (Fig. 5, bullets). The current slowly increases without any signature of impact ionization or any other threshold-type processes that can possibly cause a notable change in the 2DEG density. Because of the high density of electrons in the 2DEG channel, any possible electron injection from the contacts is estimated as insignificant ($<1\%$).

Room temperature dependence of the current on the applied electric field for $Al_{0.82}In_{0.18}N/AlN/GaN$ structures with the different AlN spacer thicknesses is illustrated in Fig. 6. At low fields, the current is governed by the product of the sheet density and the mobility (see Table I); thus it is natural that the lowest current is measured for structure 2081 when the AlN spacer is 0.3 nm thick (crossed squares). At high fields, the Ohm law no longer holds due to hot-electron effects. The results for structures 2073 (1 nm spacer, stars) 2061 (1.5 nm spacer, closed squares), and 2083 (2 nm spacer, diamonds) tend to merge at electric fields exceeding 50 kV/cm.

When the 2DEG density is independent of the bias and the electric field is uniform, the electron drift velocity v_{dr} can
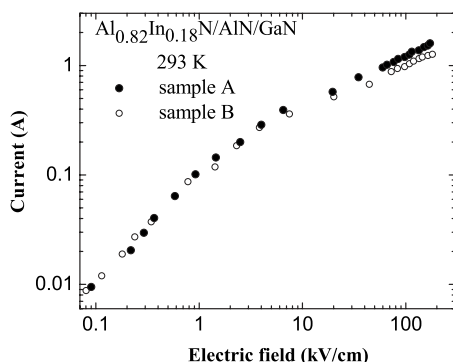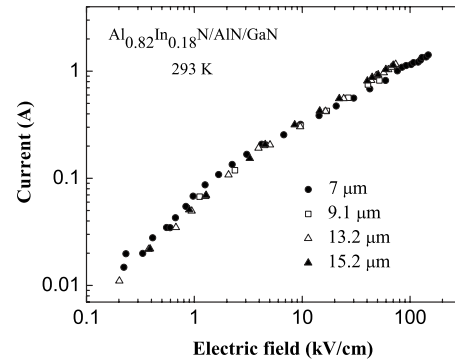

FIG. 4. Dependence of current on electric field for sample A (bullets) and sample B (open circles) of structure 2073 at room temperature. The voltage pulse duration is 1 ns, $L=5$ μm.
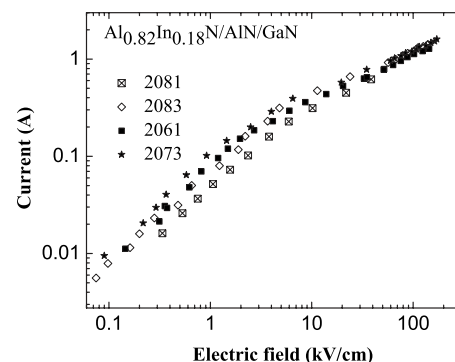

FIG. 6. Dependence of current on the electric field in the $Al_{0.82}In_{0.18}N/AlN/GaN$ channels at room temperature for structures: 2081 (crossed squares), 2083 (diamonds), 2061 (closed squares), and 2073 (stars). For spacer thickness see Table I. The voltage pulse duration is 1 ns, $L=5$ μm.
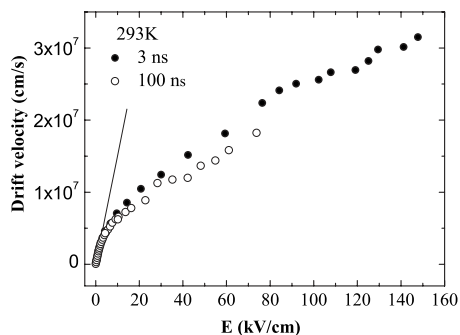
FIG. 7. Dependence on the electric field of the estimated electron drift velocity for the $Al_{0.82}In_{0.18}N/AlN/GaN$ (structure 1656) at room temperature. The duration of voltage pulses is 3 ns (bullets, present paper) and 100 ns [open circles (Ref. 29)]. The channel length is 7 μm and line is $\mu_0 E$.

be estimated from the measured current-field characteristic and the low-field mobility, μ_0. The current I_O in the Ohmic range ($E < 1.5$ kV/cm) is expressed as $I_O = C\mu_0 E$, and the normalized variable I/C, equivalent to the drift velocity $v_{dr} = \mu(E)E$, is plotted in Fig. 7 (bullets) for an $Al_{0.82}In_{0.18}N/AlN/GaN$ structure together with the $\mu_0 E$ data (solid line).

At high electric fields, no tendency for velocity saturation is observed. The highest electron drift velocity $\sim 3.2 \times 10^7$ cm/s (bullets) is reached at 150 kV/cm when the AlN spacer is 1 nm (Table I). When the same estimation is applied to another structure (2073) with a 1 nm spacer, the drift velocity is $\sim 2.2 \times 10^7$ cm/s at 150 kV/cm. The data of Fig. 6 show that the drift velocity differs only within 5% at 140 kV/cm for the structures (2073, 2083, and 2061) with different spacer thicknesses (Table I). The lowest drift velocity of $\sim 5 \times 10^6$ cm/s is attained for structure 2081 that survived only 40 kV/cm electric field. This value is more than twice lower than the value for structure 2073 ($\sim 1.2 \times 10^7$ cm/s) obtained at the same electric field.

V. DISCUSSION

The experimental results of Figs. 6 and 7 show that nanosecond pulses enabled us to reach 180 kV/cm without sample damage. No negative differential resistance (NDR) was noted, and weak dependence of the drift velocity on the spacer thickness was measured. The NDR was not observed in AlGaN/GaN structures by applying 10 ns pulses up to 140 kV/cm,[23] 1 ns voltage pulses up to 200 kV/cm,[31] and in silicon-doped GaN using a few nanosecond pulses up to 290 kV/cm.[25] On the other hand, the NDR was observed experimentally in doped GaN at 180 kV/cm (Ref. 21) when 200 ns voltage pulses were used, and in a semi-insulating undoped GaN above 320 kV/cm.[20] Channel self-heating caused the current to saturate if pulses longer than 20 ns were applied.[29] It is difficult to see NDR in quasi-dc measurements.[41] The preferred method is time of flight or microwave type measurements. On the other hand, the recent work of Ardaravičius *et al.*[42] reported on NDR in 4*H*-SiC at 280 kV/cm when a 1 ns pulsed voltage technique was used.

The NDR originates from the dependence on electric field of either the electron density or the electron mobility. Supposing that the electron density is independent of the

electric field, the NDR is associated with negative differential mobility (NDM). Calculations show that the NDM in GaN originates from either intervalley transfer or nonparabolicity of the central valley.[27] The position of the upper valleys has been recently estimated from optical experiments.[43] The NDM induced by negative effective mass is expected to appear at ~ 210 kV/cm. According to the ensemble Monte Carlo (MC) simulations, the NDM appears at electric fields about 140 kV/cm,[17,18] while full-zone MC simulation shows that the NDM in GaN appears at electric fields above 180 kV/cm.[16,28] This result disagrees with the other estimations[19] and the experimental data obtained for semi-insulating undoped GaN:[20] the threshold field for the NDM is ~ 325 kV/cm. Theoretical MC calculations incorporating a GaN full-zone band structure show that the majority of electrons do not attain sufficient energy to effect intervalley transfer until they are subjected to higher fields ($E > 325$ kV/cm).[19] So, our experiments illustrate that the electric field of 180 kV/cm is not strong enough for the intervalley transfer and the associated NDM in the investigated 2DEG channels.

The electron interaction with longitudinal optical phonons is the dominant energy relaxation mechanism in GaN 2DEG channels at moderate to high electric fields,[34] but this is not always true for the momentum scattering. The electron drift velocity is determined by the combined action of many scattering mechanisms such as impurity, alloy, interface roughness, intervalley transfer, and strain nonuniformity, just to mention a few in addition to the hot-phonon scattering. The difference between structure 2081 with smallest spacer (0.3 nm) and the other $Al_{0.82}In_{0.18}N/AlN/GaN$ structures may result from either the remote alloy scattering or the alloy scattering of the electrons transferred into the AlInN layer. A thicker (1–2 nm) AlN spacer eliminates the hot-electron transfer. As a result, the drift velocity increases.

In a 2DEG, the electron density is high and hot-phonon effects play an important role. Supposing that the hot phonons limit the electron transport, the drift velocity depends on the hot-phonon lifetime:[44,45] at a given 2DEG density, the velocity is higher if the lifetime is shorter. The recent lifetime measurement has led to the differential value of ~ 60 fs for structure 1656.[46] The obtained high value of the drift velocity of $\sim 3.2 \times 10^7$ cm/s (Fig. 7, bullets) correlates with this ultrashort lifetime of hot phonons. For comparison, the smaller value of the drift velocity, 1.7×10^7 cm/s,[31] for AlGaN/GaN structure corresponds to the hot-phonon lifetime of 350 fs.[44]

VI. CONCLUSIONS

The dependence of current on electric field is measured for LM $Al_{0.82}In_{0.18}N/AlN/GaN$ 2DEG channels when the self-heating effect is avoided. No current saturation is obtained in the investigated field range below 180 kV/cm. The highest estimated hot-electron drift velocity is $\sim 3.2 \times 10^7$ cm/s when the AlN spacer is 1 nm. This value is higher than those obtained from the earlier experiments and simulations for GaN-based 2DEG channels. At high fields, a weak (if any) dependence of the drift velocity on the spacer

thickness is found in the range from 1 to 2 nm. The relatively high velocity bodes well for high speed operation of GaN-based HFETs but the effect of the AlN spacer layer must be considered for heterostructures with thin spacers. In particular, the velocity degrades when the spacer thickness is 0.3 nm.

ACKNOWLEDGMENTS

[1] H. Morkoç, *Handbook of Nitride Semiconductors and Devices* (Wiley-VCH, Berlin, 2008), Vols. I–III.

[2] O. Ambacher, B. Foutz, J. Smart, J. R. Shealy, N. G. Weimann, K. Chu, M. Murphy, A. J. Sierakowski, W. J. Schaff, L. F. Eastman, R. Dimitrov, A. Mitchell, and M. Stutzmann, J. Appl. Phys. **87**, 334 (2000).

[3] K. Lorenz, N. Franco, E. Alves, I. M. Watson, R. W. Martin, and K. P. O'Donnell, Phys. Rev. Lett. **97**, 085501 (2006).

[4] J. Kuzmik, IEEE Electron Device Lett. **22**, 510 (2001).

[5] A. Dadgar, M. Neuburger, F. Schulze, J. Bläsing, A. Krtschil, I. Daumiller, M. Kunze, K.-M. Günther, H. Witte, A. Diez, E. Kohn, and A. Krost, Phys. Status Solidi A **202**, 832 (2005).

[6] J. Kuzmik, A. Kostopoulos, G. Konstantinidis, J.-F. Carlin, A. Georgakilas, and D. Pogany, IEEE Trans. Electron Devices **53**, 422 (2006).

[7] M. Higashiwaki, T. Mimura, and T. Matsui, Jpn. J. Appl. Phys., Part 2 **45**, L843 (2006).

[8] J. Kuzmik, G. Pozzovivo, S. Abermann, J.-F. Carlin, M. Gonshorek, E. Feltin, N. Grandjean, E. Bertagnolli, G. Strasser, and D. Pogany, IEEE Trans. Electron Devices **55**, 937 (2008).

[9] F. Medjdoub, M. Alomari, J.-F. Carlin, M. Gonshorek, E. Feltin, M. A. Py, C. Gaquiere, N. Grandjean, and E. Kohn, Electron. Lett. **44**, 696 (2008).

[10] J. Xie, X. Ni, M. Wu, J. H. Leach, Ü. Özgür, and H. Morkoç, Appl. Phys. Lett. **91**, 132116 (2007).

[11] R. Butté, J.-F. Carlin, E. Feltin, M. Gonschorek, S. Nicolay, G. Christmann, D. Simeonov, A. Castiglia, J. Dorsaz, H. J. Buehlmann, S. Christopoulos, G. Baldassarri, H. von Högersthal, A. J. D. Grundy, M. Mosca, C. Pinquier, M. A. Py, F. Demangeot, J. Frandon, P. G. Lagoudakis, J. J. Baumberg, and N. Grandjean, J. Phys. D: Appl. Phys. **40**, 6328 (2007).

[12] M. Gonschorek, J.-F. Carlin, E. Feltin, M. A. Py, and N. Grandjean, Appl. Phys. Lett. **89**, 062106 (2006).

[13] K. Jeganathan, M. Shimizu, H. Okumura, Y. Yano, and N. Akutsu, J. Cryst. Growth **304**, 342 (2007).

[14] N. Grandjean and J. Massies, Appl. Phys. Lett. **71**, 1816 (1997).

[15] Y. Cao and D. Jena, Appl. Phys. Lett. **90**, 182112 (2007).

[16] J. Kolnik, I. H. Oguzman, K. F. Brennan, R. Wang, P. P. Ruden, and Y. Wang, J. Appl. Phys. **78**, 1033 (1995).

[17] U. V. Bhapkar and M. S. Shur, J. Appl. Phys. **82**, 1649 (1997).

[18] K. F. Brennan, E. Bellotti, M. Farahmanda, J. Haralson, P. P. Ruden, J. D. Albrecht, and A. Sutandi, Solid-State Electron. **44**, 195 (2000).

[19] M. Wraback, H. Shen, E. Bellotti, J. C. Carrano, C. J. Collins, J. C. Campbell, R. D. Dupuis, M. J. Schurman, and I. T. Ferguson, Phys. Status Solidi B **228**, 585 (2001).

[20] M. Wraback, H. Shen, J. C. Carrano, C. J. Collins, J. C. Campbell, R. D. Dupuis, M. J. Schurman, and I. T. Ferguson, Appl. Phys. Lett. **79**, 1303 (2001).

[21] J. M. Barker, R. Akis, D. K. Ferry, S. M. Goodnick, T. J. Thornton, D. D. Koleske, A. E. Wickenden, and R. L. Henry, Physica B **314**, 39 (2002).

[22] M. Wraback, H. Shen, S. Rudin, E. Bellotti, M. Goano, J. C. Carrano, C. J. Collins, J. C. Campbell, and R. D. Dupuis, Appl. Phys. Lett. **82**, 3674 (2003).

[23] J. M. Barker, D. K. Ferry, D. D. Koleske, and R. J. Shul, J. Appl. Phys. **97**, 063705 (2005).

[24] E. Starikov, P. Shiktorov, V. Gružinskis, L. Varani, J. C. Vaissière, C. Palermo, and L. Reggiani, J. Appl. Phys. **98**, 083701 (2005).

[25] J. Liberis, M. Ramonas, O. Kiprijanovic, A. Matulionis, N. Goel, J. Simon, K. Wang, H. Xing, and D. Jena, Appl. Phys. Lett. **89**, 202117 (2006).

[26] S. Sridharan and P. D. Yoder, IEEE Electron Device Lett. **29**, 1190 (2008).

[27] A. Dyson and B. K. Ridley, J. Appl. Phys. **104**, 113709 (2008).

[28] S. Yamakawa, R. Akis, N. Faralli, M. Saraniti, and S. Goodnick, J. Phys.: Condens. Matter **21**, 174206 (2009).

[29] L. Ardaravičius, A. Matulionis, J. Liberis, O. Kiprijanovic, M. Ramonas, L. F. Eastman, J. R. Shealy, and A. Vertiatchikh, Appl. Phys. Lett. **83**, 4038 (2003).

[30] B. A. Danilchenko, S. E. Zelensky, E. Drok, S. A. Vitusevich, S. V. Danylyuk, N. Klein, H. Lüth, A. E. Belyaev, and V. A. Kochelap, Appl. Phys. Lett. **85**, 5421 (2004).

[31] L. Ardaravičius, M. Ramonas, O. Kiprijanovic, J. Liberis, A. Matulionis, L. F. Eastman, J. R. Shealy, X. Chen, and Y. J. Sun, Phys. Status Solidi A **202**, 808 (2005).

[32] T. Palacios, L. Shen, S. Keller, A. Chakraborty, S. Heikman, S. P. DenBaars, U. K. Mishra, J. Liberis, O. Kiprijanovic, and A. Matulionis, Appl. Phys. Lett. **89**, 073508 (2006).

[33] A. Matulionis, J. Liberis, E. Šermuksnis, J. Xie, J. H. Leach, M. Wu, and H. Morkoç, Semicond. Sci. Technol. **23**, 075048 (2008).

[34] M. Ramonas, A. Matulionis, J. Liberis, L. Eastman, X. Chen, and Y.-J. Sun, Phys. Rev. B **71**, 075324 (2005).

[35] F. Medjdoub, J.-F. Carlin, M. Gonshorek, M. A. Py, N. Grandjean, S. Vandenbrouck, C. Gaquiere, J. C. Dejaeger, and E. Kohn, Electron. Lett. **42**, 779 (2006).

[36] M. Gonschorek, J.-F. Carlin, E. Feltin, M. A. Py, N. Grandjean, V. Darakchieva, B. Monemar, M. Lorenz, and G. Ramm, J. Appl. Phys. **103**, 093714 (2008).

[37] F. Medjdoub, J.-F. Carlin, C. Gaquiere, N. Grandjean, and E. Kohn, Open Electr. Electron. Eng. J. **2**, 1 (2008).

[38] A. M. Cruz Serra and H. Abreu Santos, J. Appl. Phys. **70**, 2734 (1991).

[39] R. M. Chu, Y. G. Zhou, Y. D. Zheng, P. Han, B. Shen, and S. L. Gu, Appl. Phys. Lett. **79**, 2270 (2001).

[40] H. Y. Cha, Y. C. Choi, L. F. Eastman, M. G. Spencer, L. Ardaravičius, A. Matulionis, and O. Kiprijanovič, J. Electron. Mater. **34**, 330 (2005).

[41] P. Shaw, H. L. Grubin, and P. R. Solomon, *The Gunn-Hilsum Effect* (Academic, New York, 1979).

[42] L. Ardaravičius, A. Matulionis, O. Kiprijanovic, J. Liberis, H.-Y. Cha, L. F. Eastman, and M. G. Spencer, Appl. Phys. Lett. **86**, 022107 (2005).

[43] S. Wu, P. Geisser, J. Jun, J. Karpinski, D. Wang, and R. Sobolewski, J. Appl. Phys. **101**, 043701 (2007).

[44] A. Matulionis, J. Liberis, I. Matulionienė, M. Ramonas, L. F. Eastman, J. R. Shealy, V. Tilak, and A. Vertiatchikh, Phys. Rev. B **68**, 035338 (2003).

[45] J. Khurgin, Y. J. Ding, and D. Jena, Appl. Phys. Lett. **91**, 252104 (2007).

[46] A. Matulionis and H. Morkoç, Proc. SPIE **7216**, 721608 (2009).